Decoding cosmic origins with rays and ripples

L. Sriramkumar

Centre for Strings, Gravitation and Cosmology, Department of Physics,
Indian Institute of Technology Madras, Chennai

Ten Years of Gravitational Wave Astronomy

Indian Institute of Technology Madras, Chennai

September 14, 2025

Plan of the talk

Plan of the talk

Deepest views in space

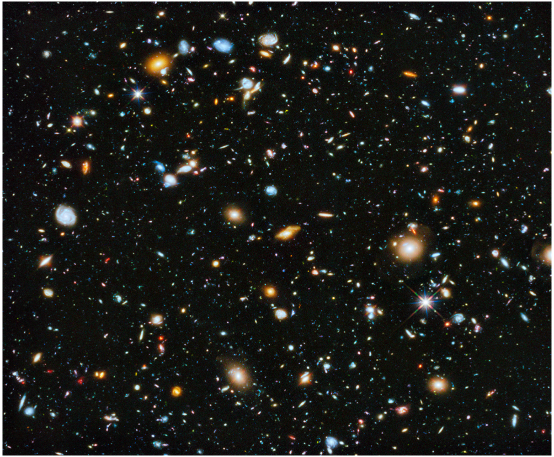

Ultra deep field images from the Hubble Space Telescope (on the left)[1] and the James Webb Space Telescope (on the right)[2].

[1] Image from http://hubblesite.org/newscenter/archive/releases/2014/27.

[2] Image from https://www.nasa.gov/image-article/nasas-webb-delivers-deepest-infrared-image-of-universe-yet/.

Distribution of galaxies in the universe

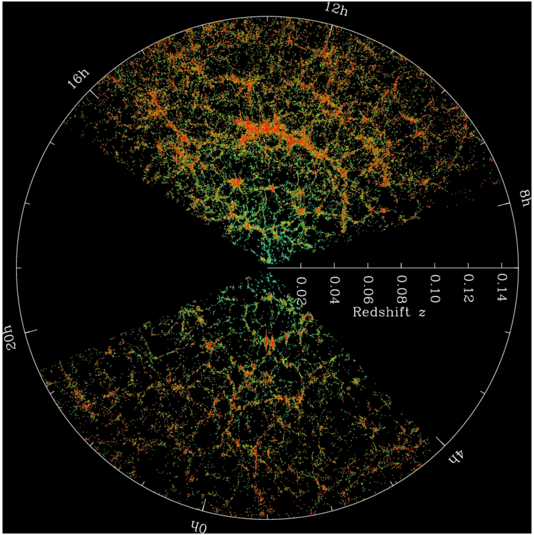

Survey by SDSS

Distribution of galaxies as observed by the Sloan Digital Sky Survey[3].

[3] Image from https://www.sdss4.org/science/.

Spectrum of radiation in the universe

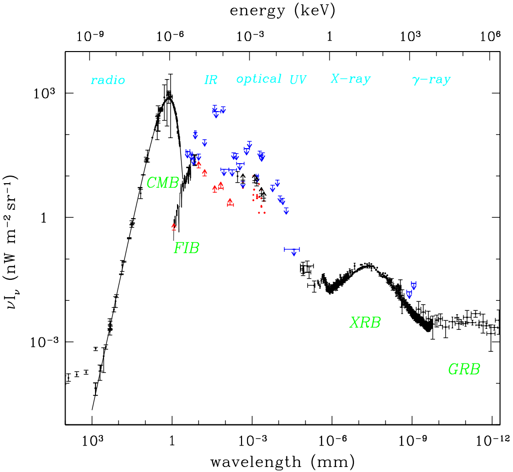

The spectrum of the cosmological background radiation has been plotted as a function of wavelength[4]. Note that the cosmic microwave background (CMB) contributes the most to the background radiation.

[4] Figure from D. Scott, arXiv:astro-ph/9912038.

Spectrum of the CMB

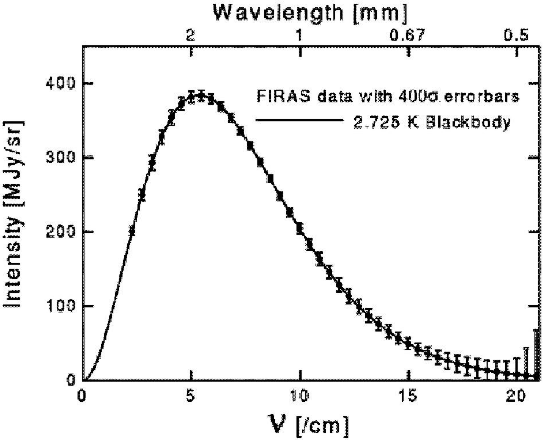

The spectrum of the CMB as measured by the COBE satellite[5]. It is such a perfect Planck spectrum (corresponding to a temperature of $2.725°$ K) that it is unlikely to be bettered in the laboratory. The error bars in the graph above have been amplified 400 times so that they can be seen!

[5] Image from http://www.astro.ucla.edu/~wright/cosmo_01.htm.

Runaway galaxies[6]

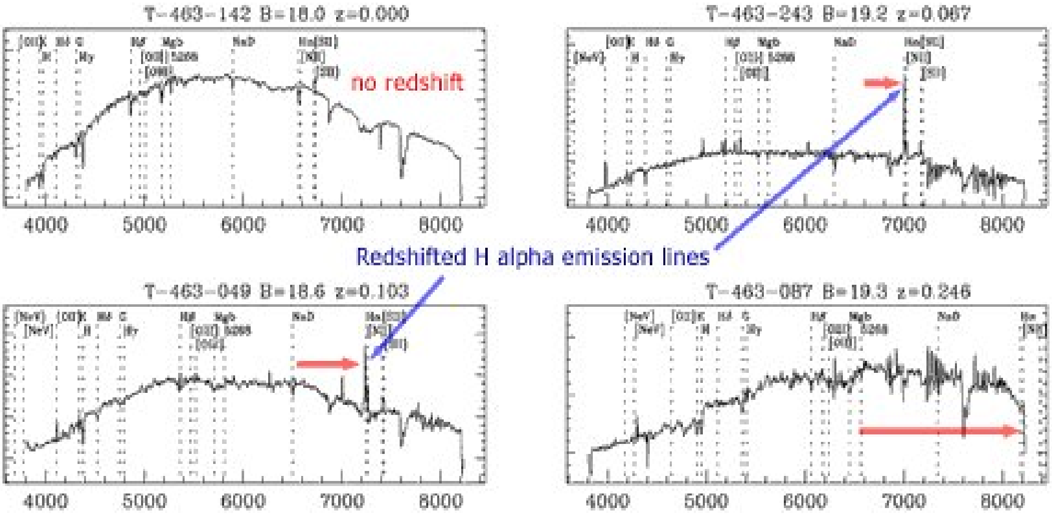

Spectra of four galaxies which exhibit redshift.

[6]Image from http://outreach.atnf.csiro.au/education/senior/astrophysics/spectra_astro_types.html.

General theory of relativity and Einstein's equations

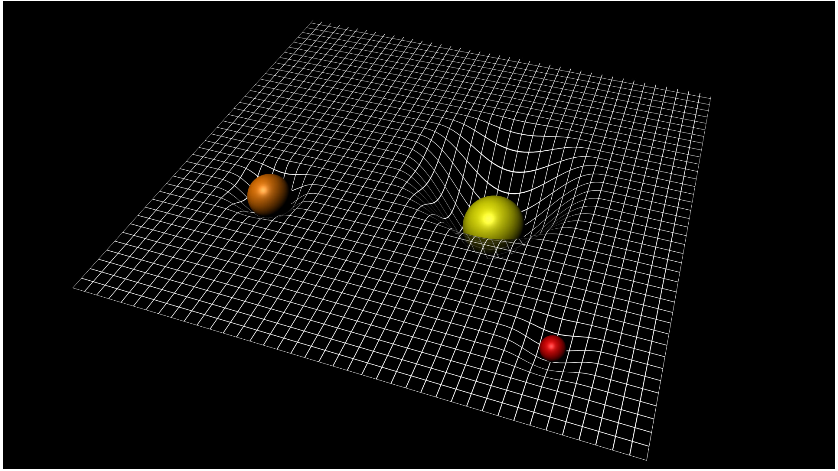

Spacetime tells matter how to move and matter tells spacetime how to curve[7]. The curvature of spacetime is related to the matter content through the Einstein's equations[8].

[7] J. A. Wheeler, *Geons, Black Holes, and Quantum Foam: A Life in Physics* (W. W. Norton, New York, 2010).

[8] Image from http://www.esa.int/spaceinimages/Images/2015/09/Spacetime_curvature.

Evolution of energy densities in the universe

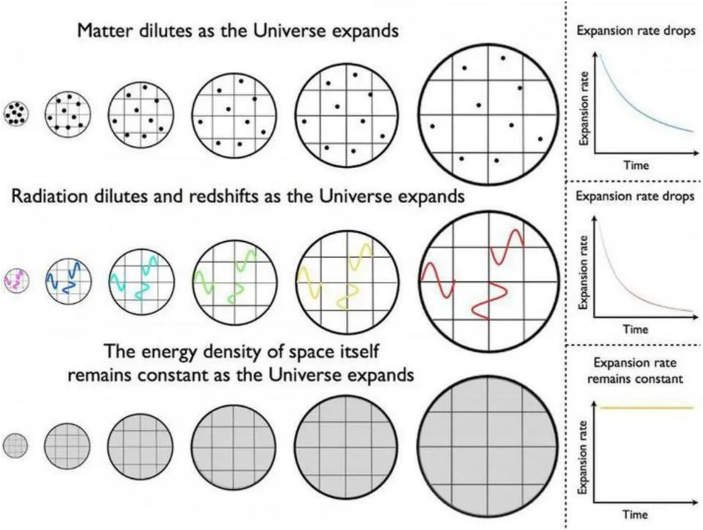

Evolution of energy densities in the universe[9].

[9] Image from https://www.forbes.com/sites/startswithabang/2021/08/25/how-small-was-the-universe-at-the-start-of-the-big-bang/.

Big bang model seems popular!

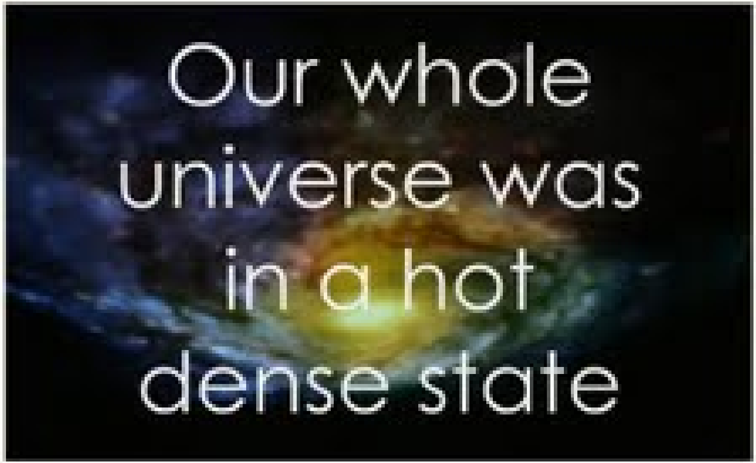

The current view of the universe, encapsulated in the hot big bang model, seems popular. The above image is a screen grab from the theme song of the recent American sitcom ‘The Big Bang Theory’[10].

[10] See http://www.cbs.com/shows/big_bang_theory/.

Decoupling of matter and radiation[11]

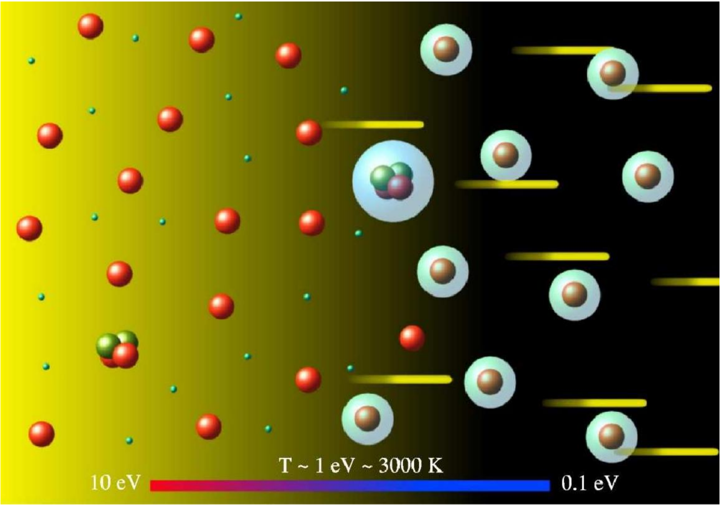

Matter and radiation cease to interact at a temperature of about $T \simeq 3000^\circ$ K, which corresponds to a redshift of about $z \simeq 1000$.

[11] Image from W. H. Kinney, arXiv:astro-ph/0301448v2.

Surface of last scattering and the free streaming of CMB photons

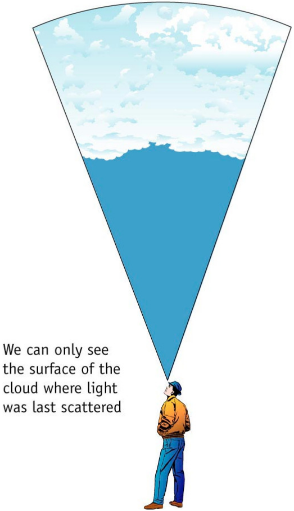

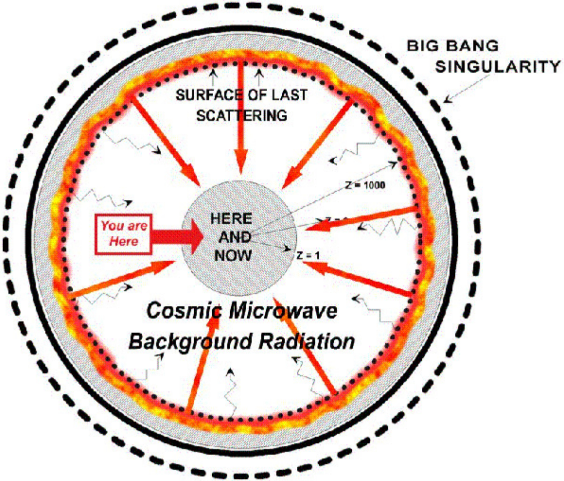

CMB photons stream to us freely from the surface of last scattering[12].

[12] Image from http://planck.caltech.edu/epo/epo-cmbDiscovery4.html.

Projecting the surface of last scattering

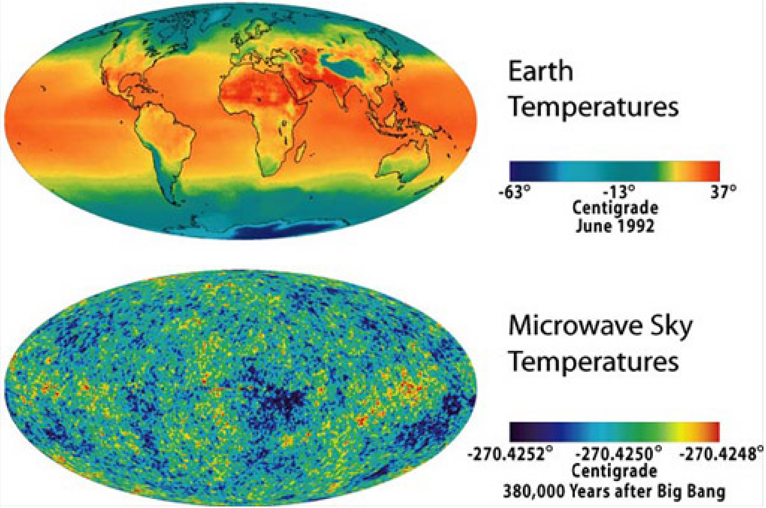

As the surface of the Earth is often illustrated, the temperature of the CMB on the surface of last scattering can be projected on to a plane using the Mollweide projection[13].

[13]Image from http://hyperphysics.phy-astr.gsu.edu/hbase/Astro/planckcmb.html.

Anisotropies in the CMB

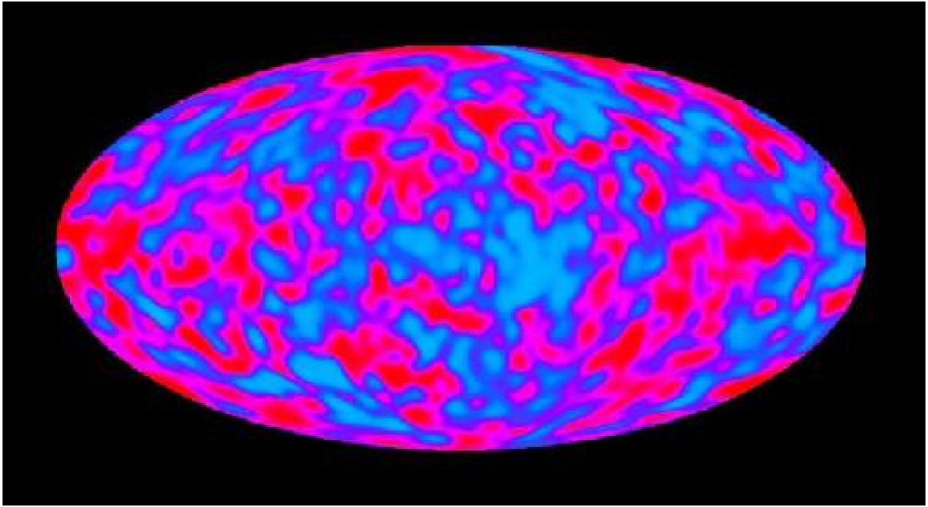

The fluctuations in the temperature of the CMB as seen by COBE[14]. The CMB turns out to be isotropic to one part in 10^5.

[14] Image from http://aether.lbl.gov/www/projects/cobe/COBE_Home/DMR_Images.html.

Anisotropies in the CMB as seen by WMAP and Planck

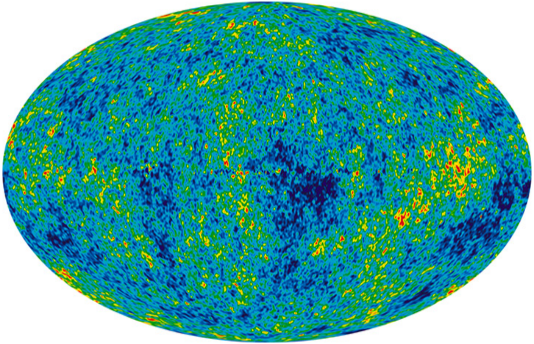

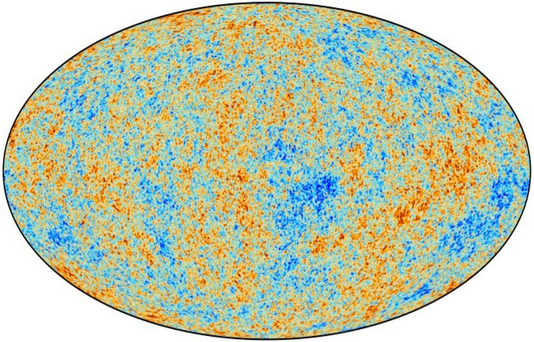

Left: All-sky map of the anisotropies in the CMB created from nine years of Wilkinson Microwave Anisotropy Probe (WMAP) data[15].
Right: CMB intensity map derived from the joint analysis of Planck, WMAP, and $408\,\mathrm{MHz}$ observations[16]. The above images show temperature variations (as color differences) of the order of $200\,\mu\mathrm{K}$.

[15] Image from http://wmap.gsfc.nasa.gov/media/121238/index.html.

[16] P. A. R. Ade *et al.*, arXiv:1502.01582 [astro-ph.CO].

Plan of the talk

Horizon problem

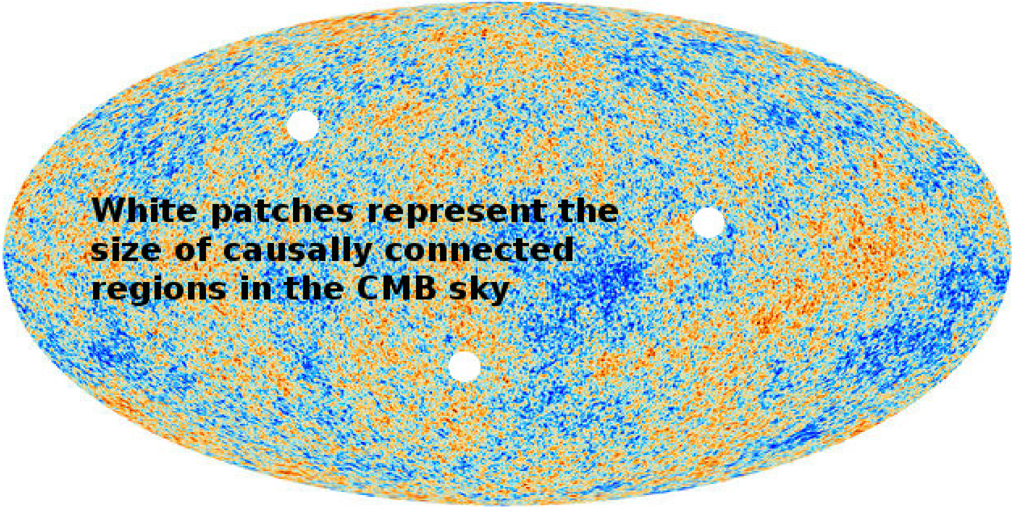

The radiation from the CMB arriving at us from regions separated by more than the Hubble radius at the surface of last scattering, which subtends an angle of about 1° today, could not have interacted before decoupling.

Resolution of the horizon problem in the inflationary scenario

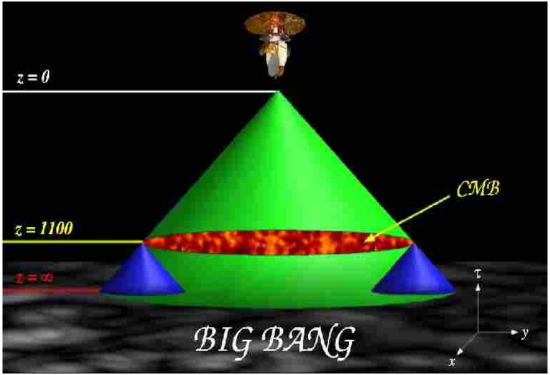

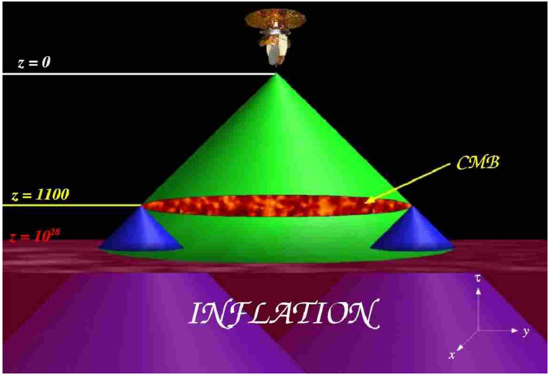

Another illustration of the horizon problem (on the left), and an illustration of its resolution (on the right) through an early and sufficiently long epoch of inflation[17].

[17] Images from W. Kinney, astro-ph/0301448.

Time and duration of inflation

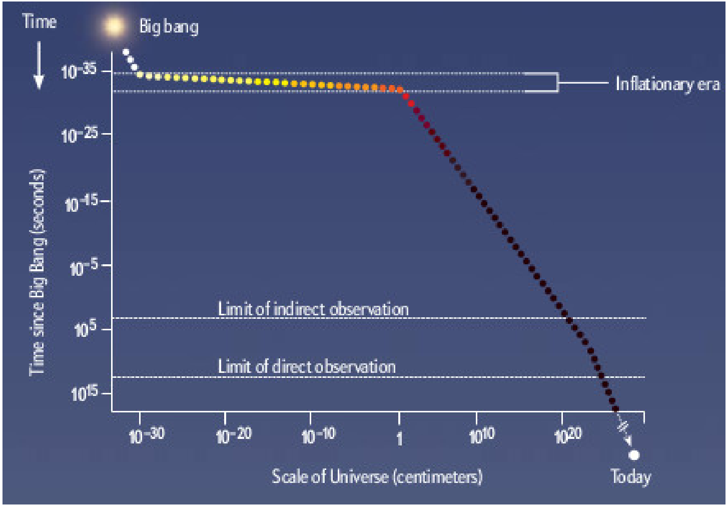

Inflation—a brief period of accelerated expansion—is expected to have taken place during the very early stages of the universe[18].

[18] Image from P. J. Steinhardt, Sci. Am. **304**, 18 (2011).

Inflationary attractor

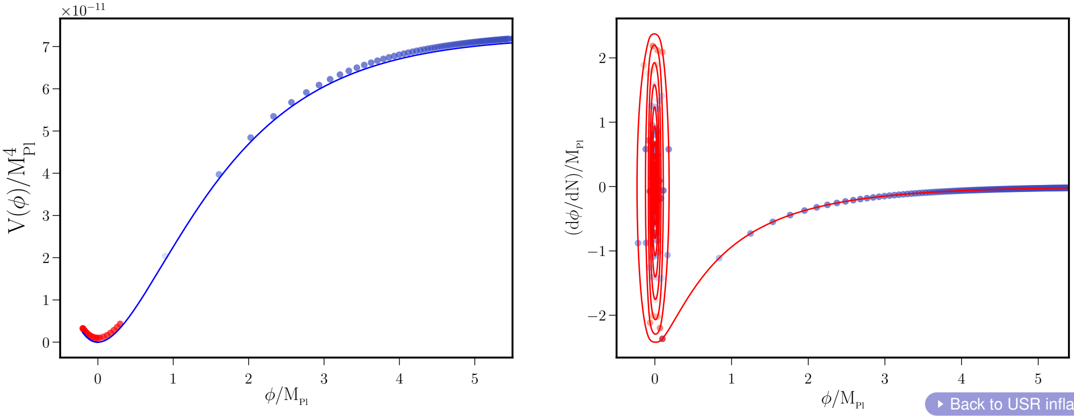

Back to USR inflation

Evolution of the scalar field in the popular Starobinsky model, which leads to slow roll inflation, is indicated (as circles, in blue and red) at regular intervals of time (on the left). Illustration of the behavior of the scalar field in phase space (on the right)[19].

[19] Figure from H. V. Ragavendra, *Observational imprints of non-trivial inflationary dynamics over large and small, scales*, Ph.D. Thesis, Indian Institute of Technology Madras, Chennai, India (2022).

Origin and evolution of the primordial perturbations

- The quantum fluctuations associated with the scalar fields that drive inflation are responsible for the origin of the primordial perturbations.
- The perturbations in the metric and matter are related through the Einstein's equations.
- The scalar perturbations, say, the perturbations in the energy density and pressure of matter, leave the largest imprints on the CMB. They are also primarily responsible for the inhomogeneities in the distribution of matter in the universe at later epochs.
- Note that, the tensor perturbations in the metric, i.e. gravitational waves (GWs) or ripples in spacetime, can be generated even in the absence of sources.

Play movie

Behavior of the comoving wave number and Hubble radius

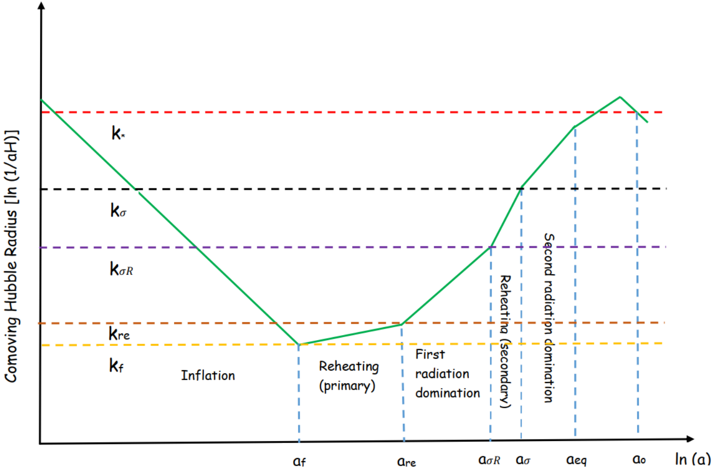

Back to reheating
Back to formation of PBHs
Back to secondary GWs

Behavior of the comoving wave number k (horizontal lines in different colors) and the comoving Hubble radius $d_{\mathrm{H}}/a = (a\,H)^{-1}$ (in green) across different epochs[20].

[20] Md. R. Haque, D. Maity, T. Paul and L. Sriramkumar, Phys. Rev. D **104**, 063513 (2021).

Essential properties of GWs

- The GWs are small disturbances in a given spacetime (very much like ripples in water), which travel at the speed of light.
- They satisfy the wave equation in the given background spacetime.
- The GWs are transverse in nature and are characterized by two degrees of polarization[21].

[21] J. B. Hartle, *Gravity: An Introduction to Einstein's General Relativity* (Pearson Education, Delhi, 2003).

Polarization of GWs

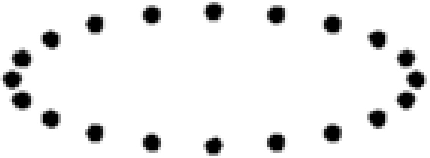

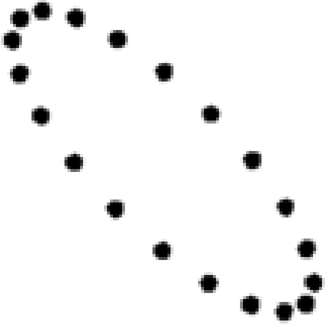

A GW impinging on a ring of masses leads to oscillations of the particles depending on the polarization of the wave: plus (on the left) and cross (on the right)[22].

[22] J. B. Hartle, *Gravity: An Introduction to Einstein's General Relativity* (Pearson Education, Delhi, 2003).

Describing the primordial perturbations

While comparing with the observations, for convenience, one often uses the following power law, template scalar and the tensor spectra[23]:

$$\mathcal{P}_{_{\rm S}}(k) = A_{_{\rm S}}\,\left(\frac{k}{k_\ast}\right)^{n_{_{\rm S}}-1}, \qquad \mathcal{P}_{_{\rm T}}(k) = A_{_{\rm T}}\,\left(\frac{k}{k_\ast}\right)^{n_{_{\rm T}}},$$

where $A_{_{\rm S}}$ and $A_{_{\rm T}}$ denote the scalar and tensor amplitudes, $k_\ast$ represents the so-called pivot scale at which the amplitudes are quoted, while the spectral indices $n_{_{\rm S}}$ and $n_{_{\rm T}}$ are assumed to be constant.

The tensor-to-scalar ratio r is defined as

$$r(k) = \frac{\mathcal{P}_{_{\rm T}}(k)}{\mathcal{P}_{_{\rm S}}(k)}.$$

[23] See, for instance, L. Sriramkumar, Curr. Sci. **97**, 868 (2009).

Plan of the talk

CMB angular power spectrum from Planck

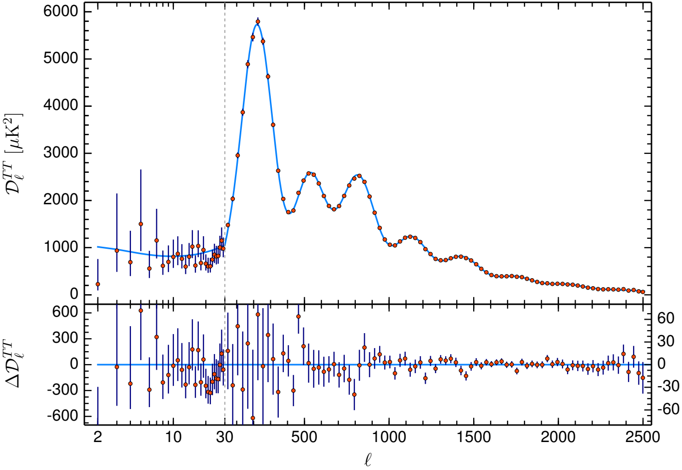

The CMB TT angular power spectrum from the Planck 2018 data (red dots with error bars) and the best fit ΛCDM model with a power law primordial spectrum (solid blue curve)[24]

[24] Planck Collaboration (N. Aghanim *et al.*), Astron. Astrophys. **641**, A6 (2020).

Performance of inflationary models in the $n_{\rm s}$-r plane

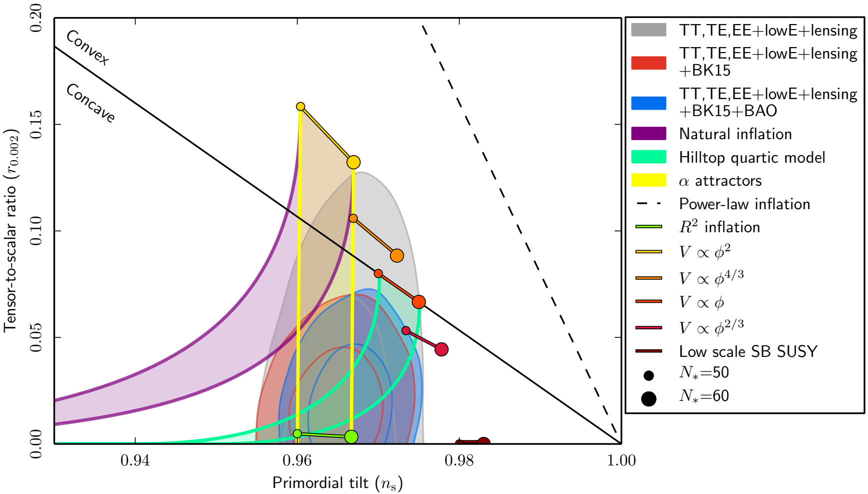

Joint constraints on $n_{\rm s}$ and $r_{0.002}$ from Planck in combination with other data sets, compared to the theoretical predictions of some of the popular inflationary models[25].

[25] Planck Collaboration (Y. Akrami *et al.*), Astron. Astrophys. **641**, A10 (2020).

Polarization of the CMB

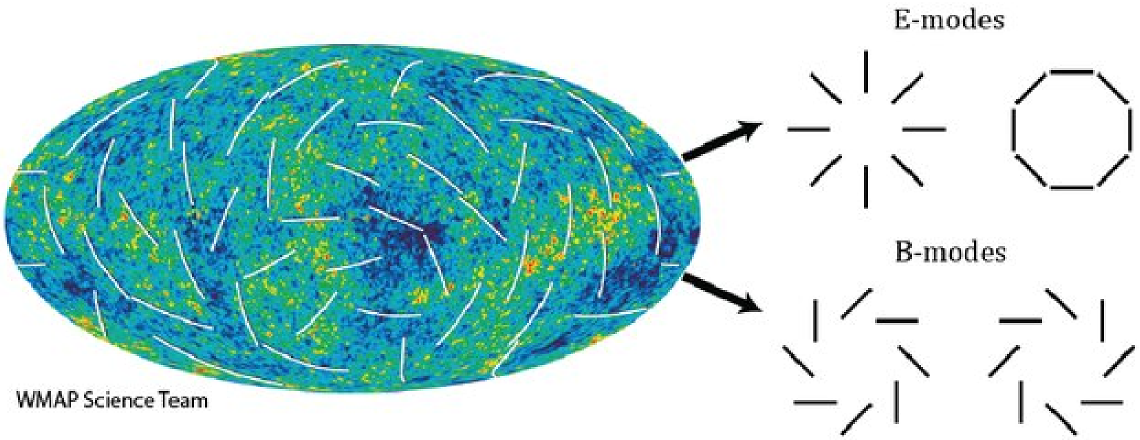

E-mode and B-mode polarizations of the CMB[26]. On large scales, the B-modes are generated by primordial GWs.

[26] See, for instance, J. Lazear *et al.*, arXiv:1407.2584 [astro-ph.IM].

Status of observations of the B-mode polarization of the CMB

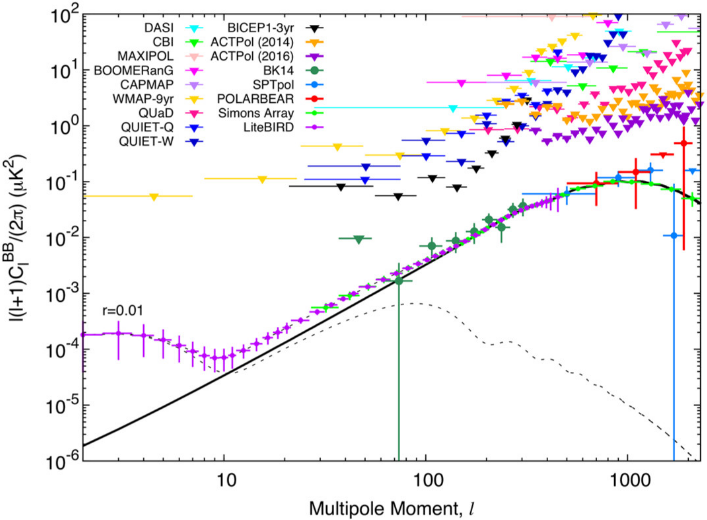

Upper limits on the B-mode polarization of the CMB[27].

[27] See M. Hazumi *et al.*, J. Low Temp. Phys. **194**, 443 (2019).

Prospects of observing the imprints of the tensor perturbations

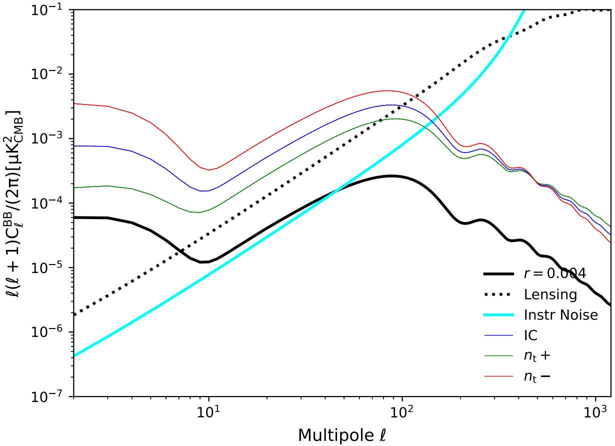

The B-mode angular power spectra of the CMB resulting from the primordial tensor perturbations for three models with $r_{0.05} = 0.05$ have been plotted, along with the CMB lensing signal and the instrumental noise of a LiteBIRD-like configuration[28].

[28] D. Paoletti, F. Finelli, J. Valiviita and M. Hazumi, Phys. Rev. D **106**, 083528 (2022).

Timeline of the universe I

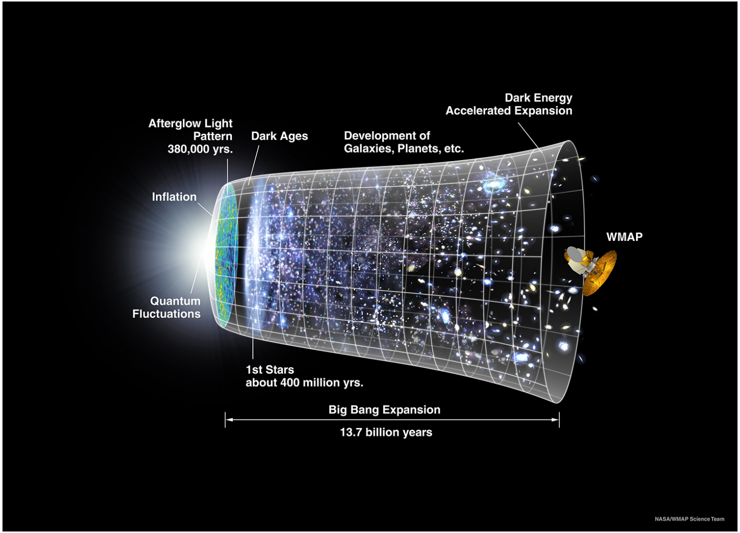

Observations of GWs

A pictorial timeline of the universe[29].

[29] See http://wmap.gsfc.nasa.gov/media/060915/060915_CMB_Timeline150.jpg.

Timeline of the universe II

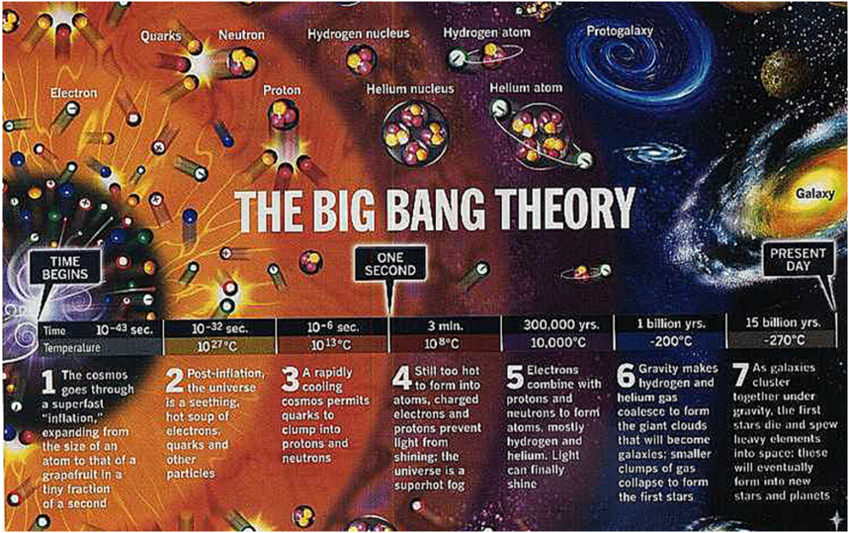

A more dramatic timeline of the universe[30]!

[30] Image from https://altexploit.wordpress.com/2017/05/20/without-explosions-we-would-not-exist/.

Plan of the talk

Laser Interferometer Gravitational-Wave Observatory (LIGO)

Views of LIGO at Hanford (on the left) and at Livingston (on the right). These observatories are essentially Michelson-Morley interferometers with rather long arms (of length about 4 km) that are extremely sensitive to the smallest disturbances of the mirrors[31].

[31] Images from https://www.advancedligo.mit.edu/summary.html.

GWs from merging binary black holes

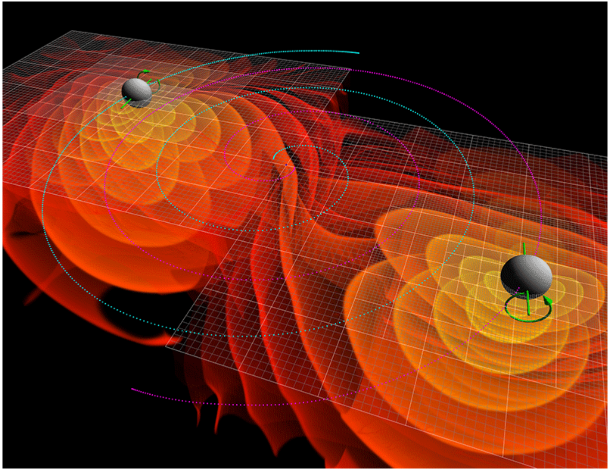

Numerical simulations of the GWs emitted by the coalescence of two black holes. The orange contours represent the amplitude of the GWs and the blue lines represent the orbits of the black holes (BHs)[32].

[32] Image from E. Berti, Physics **9**, 17 (2016).

First observation of merging binary BHs

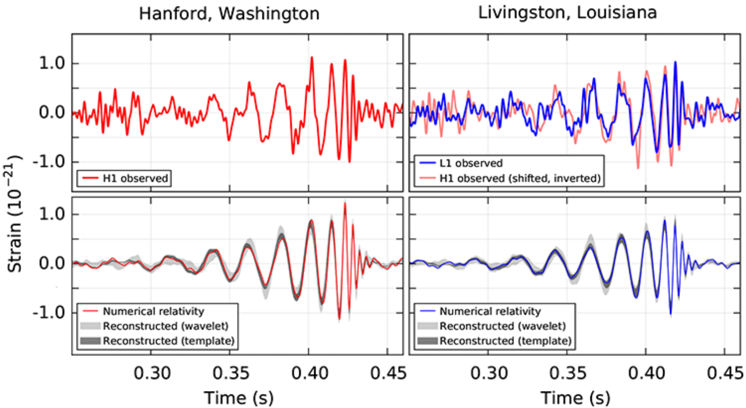

On September 14, 2015, similar signals were observed in both of LIGO's interferometers. The top panels show the measured signal in the Hanford (top left) and Livingston (top right) detectors. The bottom panels show the expected signal produced by the merger of two BHs, based on numerical simulations[33].

[33] Figure from B. P. Abbott *et al.*, Phys. Rev. Lett. **116**, 061102 (2016).

Sources and spectral range of GWs I

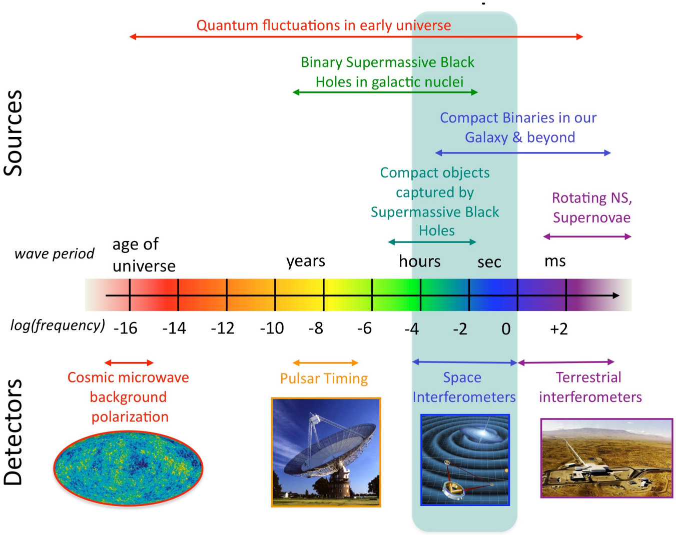

Different sources of GWs and corresponding detectors[34].

[34] J. B. Hartle, *Gravity: An Introduction to Einstein's General Relativity* (Pearson Education, Delhi, 2003).

Sources and spectral range of GWs II

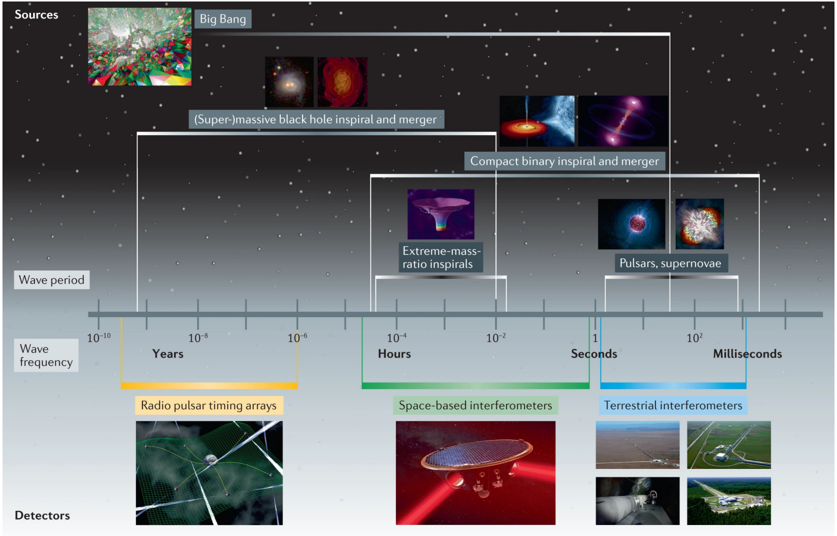

Another image of sources of GWs and detectors[35].

[35] M. Bailes *et al.*, Nat. Rev. Phys. **3**, 344 (2021).

Probing the primordial universe through GWs

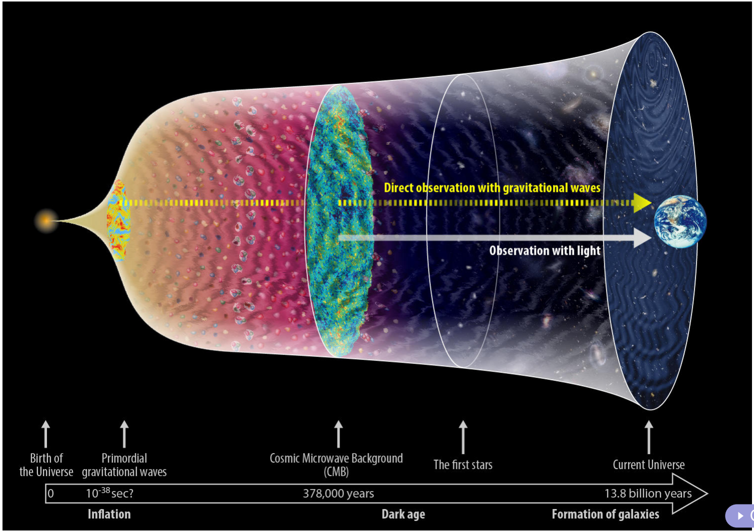

Observations of EM waves

GWs provide a unique window to probe the primordial universe[36].

[36] Image from https://gwpo.nao.ac.jp/en/gallery/000061.html.

Plan of the talk

Evolution of the scalar field in an inflationary potential

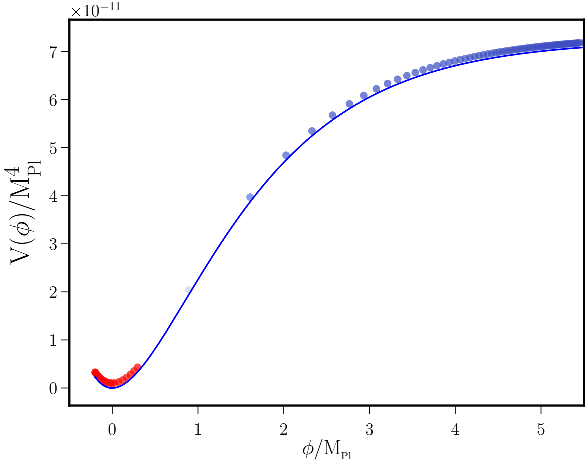

The evolution of the scalar field in the so-called Starobinsky model has been indicated (as circles, in blue and red) at regular intervals of time. Inflation is terminated as the field approaches the bottom of the potential (near the light blue dot). Thereafter, the field oscillates at the bottom of the potential (indicated by the red dots).

Effects on primary $\Omega_{\rm GW}(f)$ due to secondary reheating

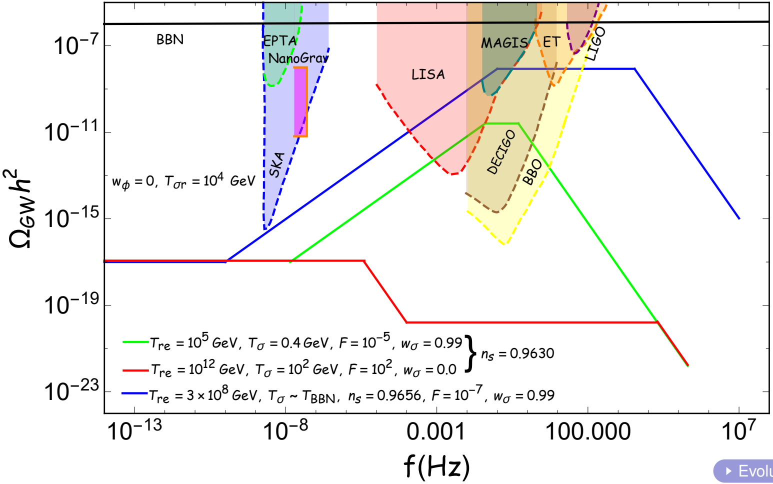

Evolution of comoving lengths

The dimensionless spectral energy density of primary GWs observed today $\Omega_{\rm GW}(f)$ has been plotted in a scenario involving a secondary phase of reheating[37].

[37] Md. R. Haque, D. Maity, T. Paul and L. Sriramkumar, Phys. Rev. D **104**, 063513 (2021).

Coalescence of compact binaries observed by LIGO

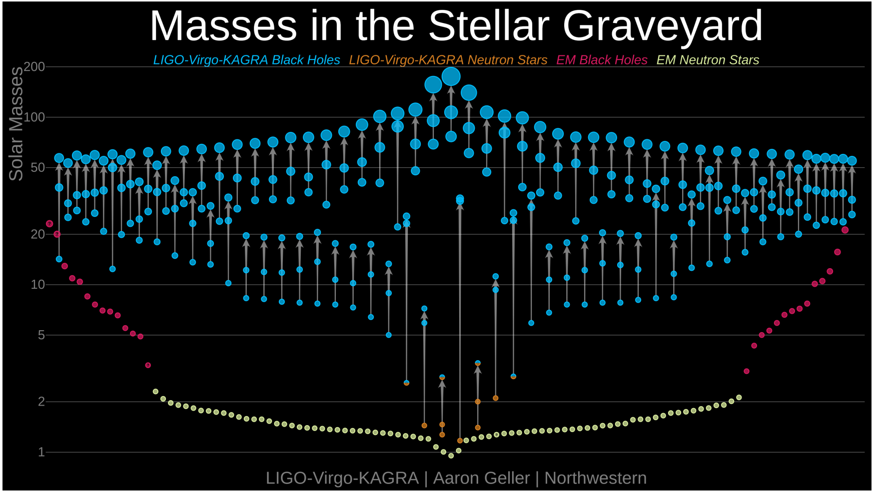

The third GW Transient Catalog of mergers involving black holes and neutron stars observed by the LIGO-Virgo-KAGRA collaboration[38].

[38] Image from https://www.ligo.caltech.edu/LA/image/ligo20211107a.

Formation of BHs in the early universe

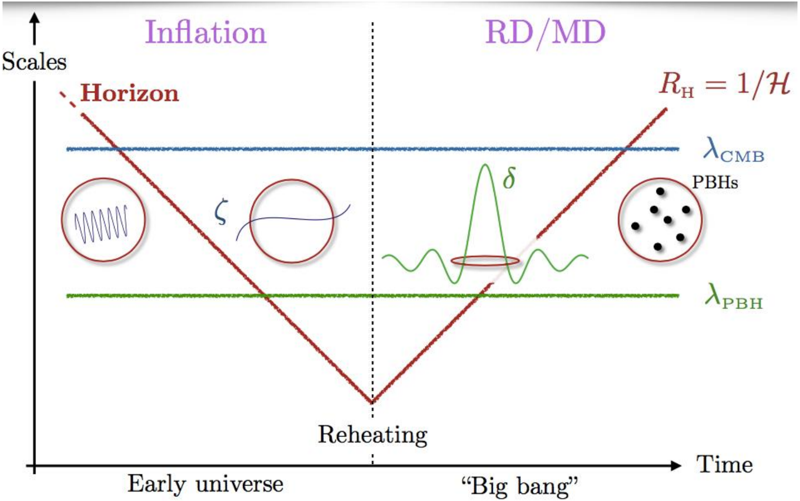

BHs can form when perturbations with significant amplitudes reenter the Hubble radius during the radiation dominated epoch[39].

Evolution of comoving lengths

[39] Figure from G. Franciolini, arXiv:2110.06815 [astro-ph.CO].

Amplitude required to form significant number of PBHs

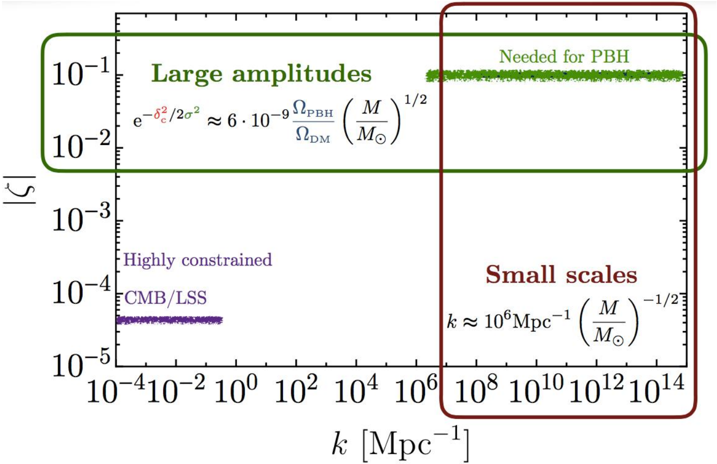

In order to form significant number of primordial black holes (PBHs), the amplitude of the perturbations on small scales has to be large enough such that the dimensionless amplitude of the scalar perturbation is close to unity[40].

[40] Figure credit G. Franciolini.

Single-field models admitting ultra slow roll inflation

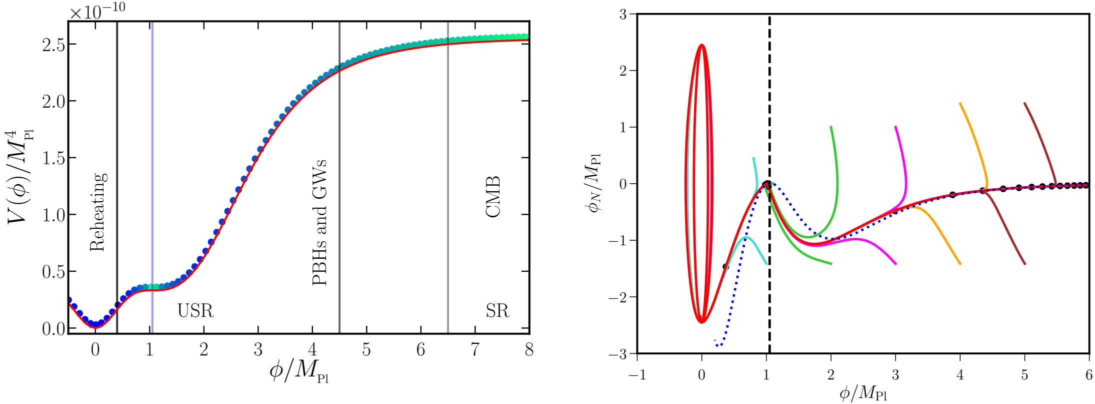

▸ Inflationary attractor

Potentials which contain a point of inflection lead to ultra slow roll (USR) inflation[41].

[41] See, for example, C. Germani and T. Prokopec, Phys. Dark Univ. **18**, 6 (2017); I. Dalianis, A. Kehagias and G. Tringas, JCAP **01**, 037 (2019). Figures credits, H. V. Ragavendra and S. Maity.

Power spectra in models permitting USR inflation

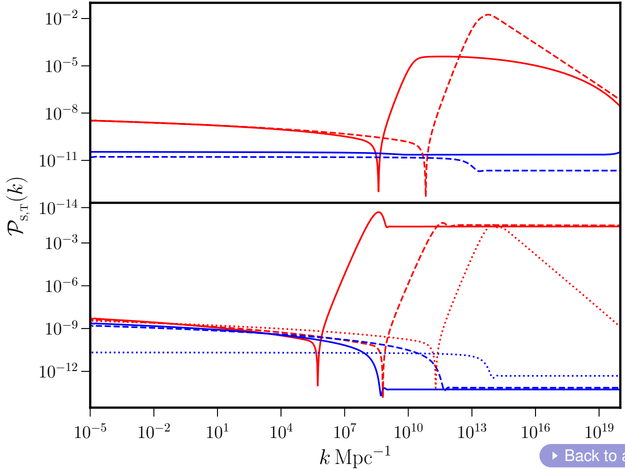

Back to analytical form of the power spectrum

Scalar (in red) and the tensor (in blue) power spectra arising in different single-field models that permit a period of USR inflation[42].

[42] H. V. Ragavendra, P. Saha, L. Sriramkumar and J. Silk, Phys. Rev. D **103**, 083510 (2021); Also see H. V. Ragavendra and L. Sriramkumar, Galaxies **11**, 34 (2023).

Non-trivial inflationary dynamics in a two-field model of inflation

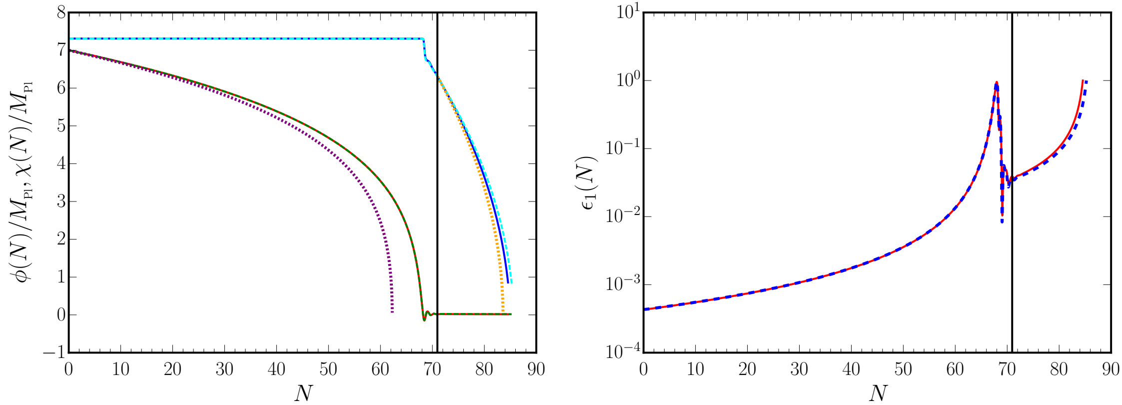

Behavior of the two scalar fields ϕ and χ (in blue and red, on the left) and the first slow roll parameter ϵ_1 (on the right) in the two field model of our interest[43]. Note that there arises a turn in the field space around $N = 70$, when the first slow roll parameter begins to decrease before increasing again, leading to the termination of inflation.

[43] M. Braglia, D. K. Hazra, F. Finelli, G. F. Smoot, L. Sriramkumar and A. A. Starobinsky, JCAP **08**, 001 (2020).

Enhanced power on small scales in the two-field model

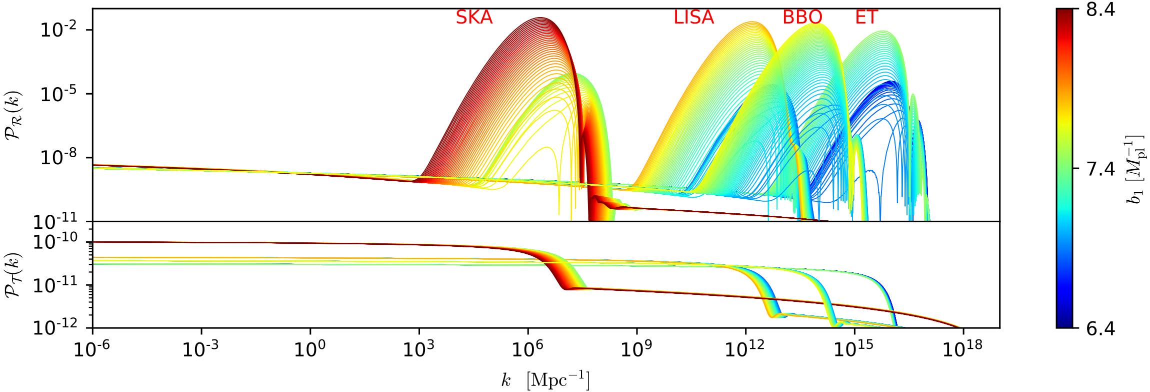

The scalar (on top) and the tensor (at the bottom) power spectra evaluated at the end of inflation have been plotted for a few different sets of initial conditions for the fields and a range of values of a particular parameter[44].

[44] M. Braglia, D. K. Hazra, F. Finelli, G. F. Smoot, L. Sriramkumar and A. A. Starobinsky, JCAP **08**, 001 (2020).

$f_{\rm PBH}(M)$ in models permitting USR inflation

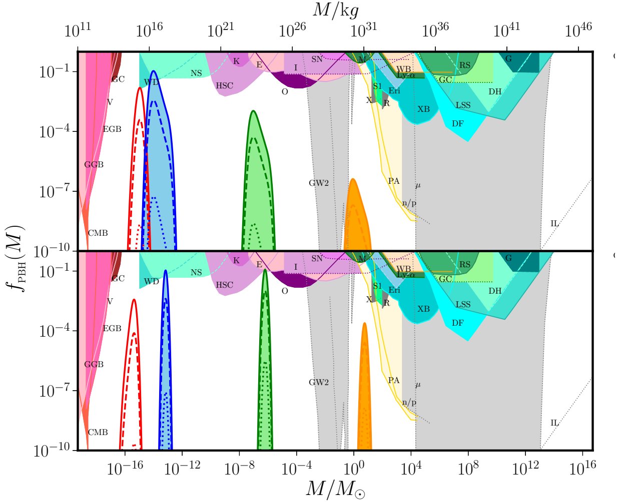

The fraction of PBHs contributing to the dark matter density today $f_{\rm PBH}(M)$ has been plotted for different models and scenarios of interest[45].

[45] H. V. Ragavendra, P. Saha, L. Sriramkumar and J. Silk, Phys. Rev. D **103**, 083510 (2021).

$f_{\rm PBH}(M)$ in the two-field model

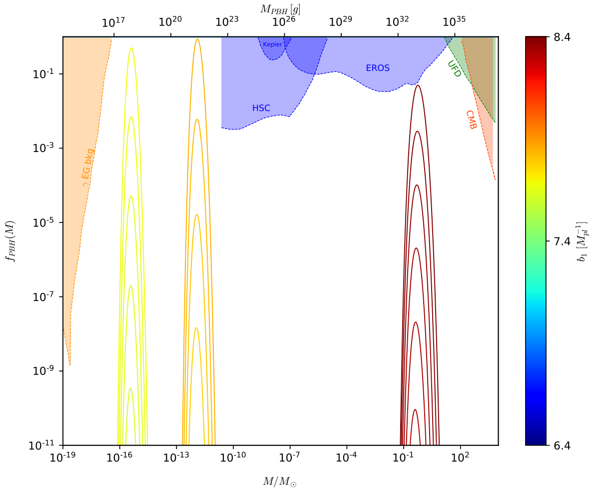

The fraction of PBHs contributing to the dark matter density today $f_{\rm PBH}(M)$ in the two-field model of our interest[46].

[46] M. Braglia, D. K. Hazra, F. Finelli, G. F. Smoot, L. Sriramkumar and A. A. Starobinsky, JCAP **08**, 001 (2020).

Secondary $\Omega_{\rm GW}(f)$ in models permitting USR inflation

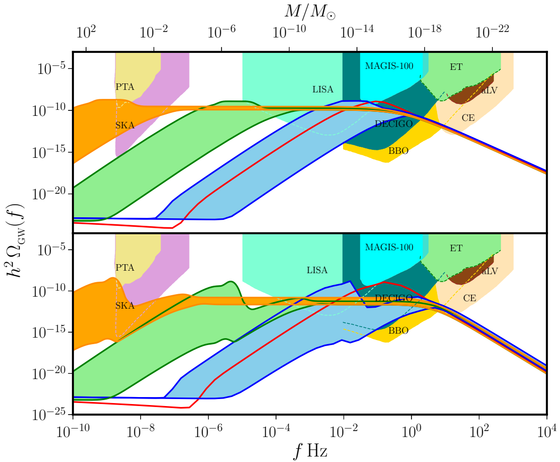

The dimensionless spectral energy density of secondary GWs today $\Omega_{\rm GW}$ arising in the models and reconstructed scenarios leading to an epoch of ultra slow roll inflation has been plotted as a function of the frequency f[47].

[47] H. V. Ragavendra, P. Saha, L. Sriramkumar and J. Silk, Phys. Rev. D **103**, 083510 (2021).

Secondary $\Omega_{\rm GW}(f)$ in the two-field model

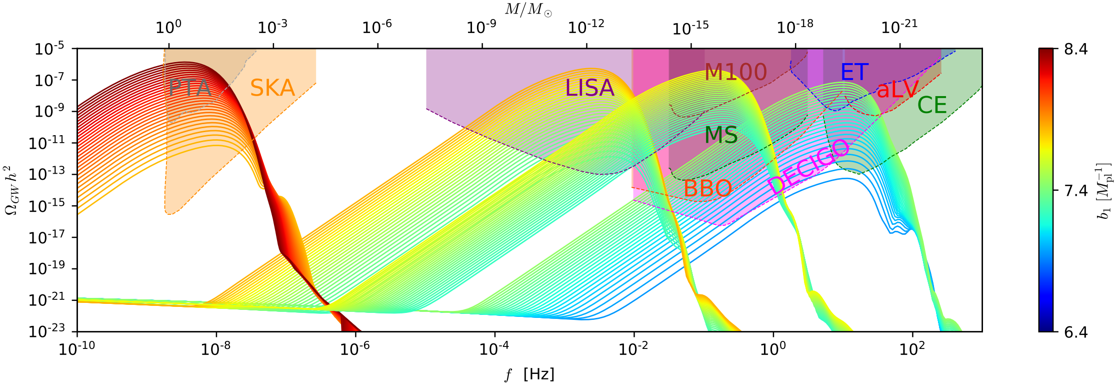

The dimensionless spectral energy density of secondary GWs today $\Omega_{\rm GW}(f)$ arising in the two-field model of inflation has been plotted for a set of initial conditions for the background fields as well as a range of values of a parameter describing the model[48].

[48] M. Braglia, D. K. Hazra, F. Finelli, G. F. Smoot, L. Sriramkumar and A. A. Starobinsky, JCAP **08**, 001 (2020).

Plan of the talk

Pulsars

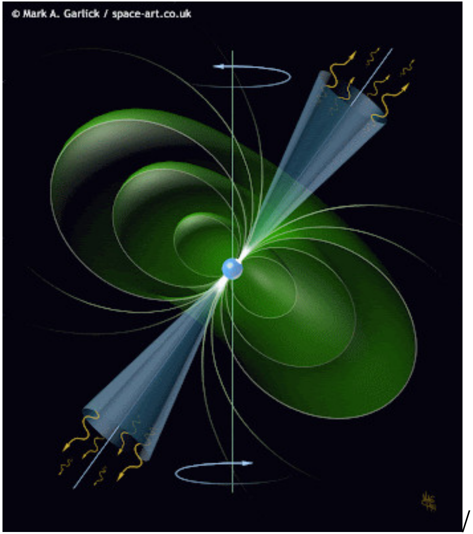

Pulsars are dense and rotating neutron stars that emit regular beams of light[49].

[49] Image from https://dmr-astronomersclub.blogspot.com/2012/07/what-is-pulsar.html.

Pulsar timing arrays

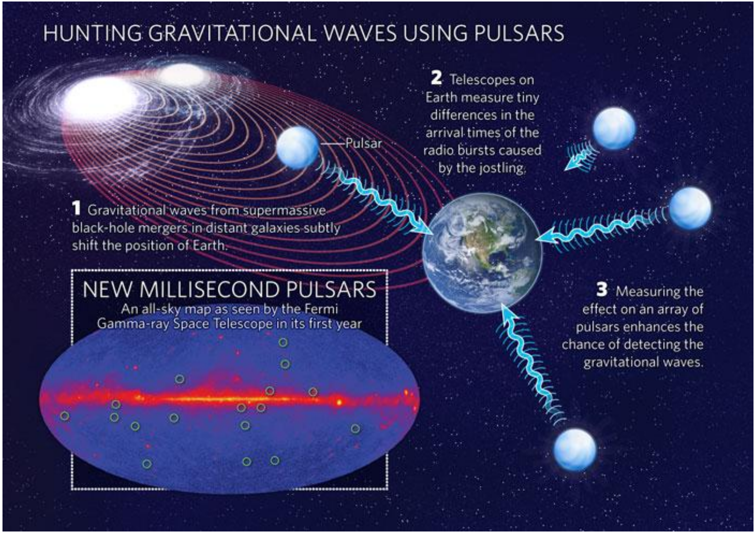

The Pulsar timing arrays (PTAs) monitor an array of millisecond pulsars[50].

[50] See https://ipta.github.io/mock_data_challenge/.

Hellings-Downs curve

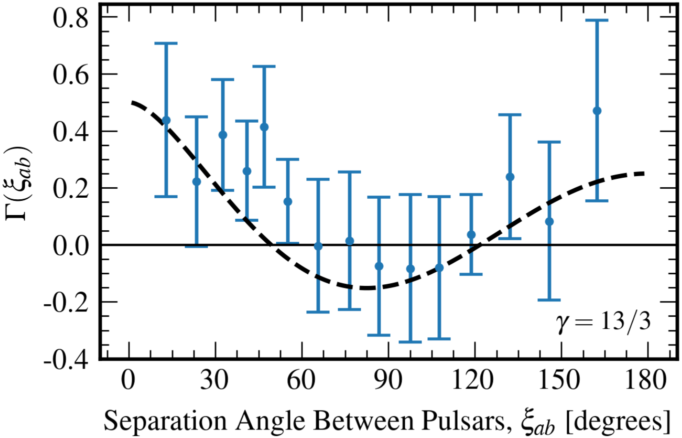

The inter-pulsar correlations measured from 2,211 distinct pairings in the 67-pulsar array of the NANOGrav 15-year data. The dashed black line shows the Hellings-Downs correlation pattern[51].

[51] NANOGrav Collaboration (G. Agazie *et al.*), Astrophys. J. Lett. **951**, 1 (2023).

Constraints on the spectral amplitude and index of GWs

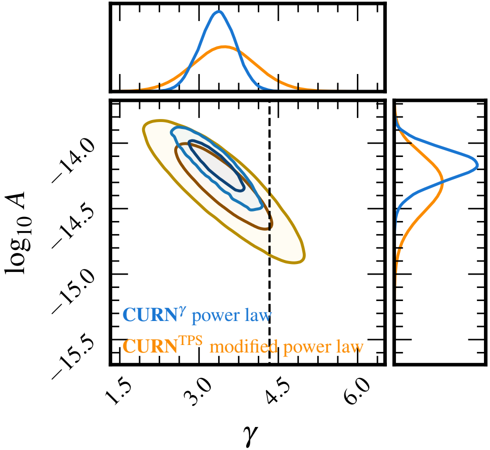

Constraints on the amplitude A and the index γ of the stochastic background of GWs from the NANOGrav 15-year data[52].

[52] NANOGrav Collaboration (G. Agazie *et al.*), Astrophys. J. Lett. **951**, 1 (2023).

Stochastic GW background observed by PTAs

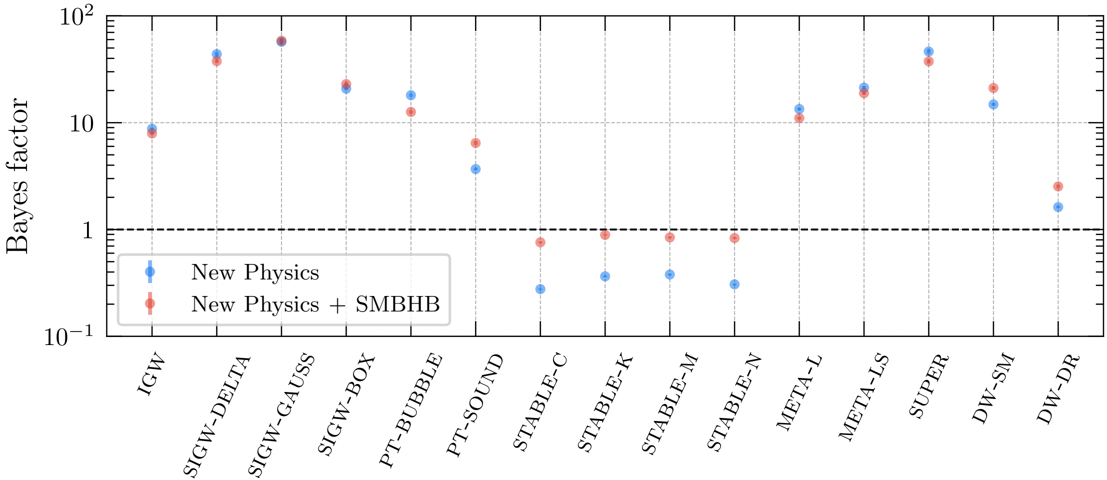

The Bayesian evidence for a variety of astrophysical and cosmological sources for the stochastic GW background suggested by the observations of the PTAs[53].

[53] NANOGrav Collaboration (G. Agazie *et al.*), Astrophys. J. Lett. **951**, 1 (2023).

Shape of the inflationary scalar power spectrum

We assume that the inflationary scalar power spectrum is given by[54]

$$\mathcal{P}_{\mathrm{S}}(k) = A_{\mathrm{S}} \left(\frac{k}{k_*}\right)^{n_{\mathrm{S}}-1} + A_0 \begin{cases} \left(\dfrac{k}{k_{\mathrm{peak}}}\right)^4 & k \leq k_{\mathrm{peak}}, \\ \left(\dfrac{k}{k_{\mathrm{peak}}}\right)^{n_0} & k \geq k_{\mathrm{peak}}, \end{cases}$$

where A_{S} and n_{S} are the amplitude and spectral index of the power spectrum at the CMB pivot scale of $k_* = 0.05\,\mathrm{Mpc}^{-1}$.

Power spectra in USR inflation

We set the reheating temperature to the rather low value of $T_{\mathrm{re}} = 50\,\mathrm{MeV}$.

We shall assume that the threshold value of the density contrast for the formation of PBHs is given by[55]:

$$\delta_{\mathrm{c}}^{\mathrm{an}} = \frac{3\,(1+w_{\mathrm{re}})}{5+3\,w_{\mathrm{re}}}\,\sin^2\left(\frac{\pi\,\sqrt{w_{\mathrm{re}}}}{1+3\,w_{\mathrm{re}}}\right).$$

[54] For other forms of spectra, see G. Domènech, S. Pi, A. Wang and J. Wang, arXiv:2402.18965 [astro-ph.CO].

[55] In this context, see T. Harada, C.-M. Yoo, and K. Kohri, Phys. Rev. D **88**, 084051 (2013).

Constraints on the epoch of reheating

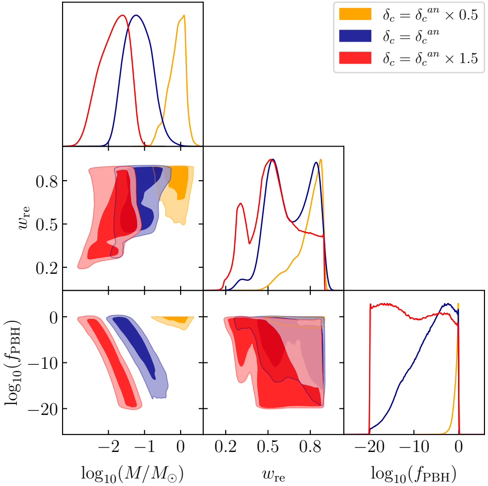

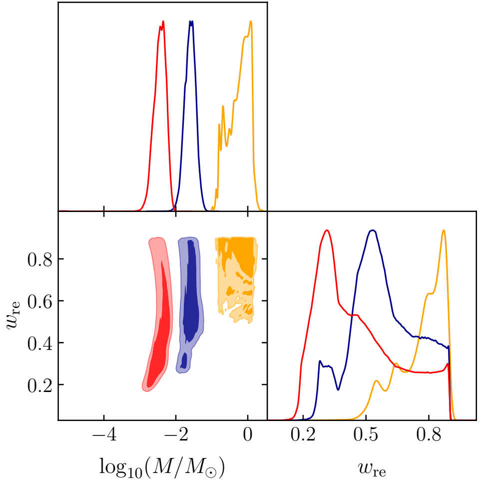

Constraints on the parameters in the models `R3pB` (on the left) and `R2pB` (on the right), arrived at upon comparison with the NANOGrav 15-year data[56].

[56] S. Maity, N. Bhaumik, Md. R. Haque, D. Maity and L. Sriramkumar, JCAP **01**, 118 (2025).

Generation of secondary GWs during the epoch of reheating

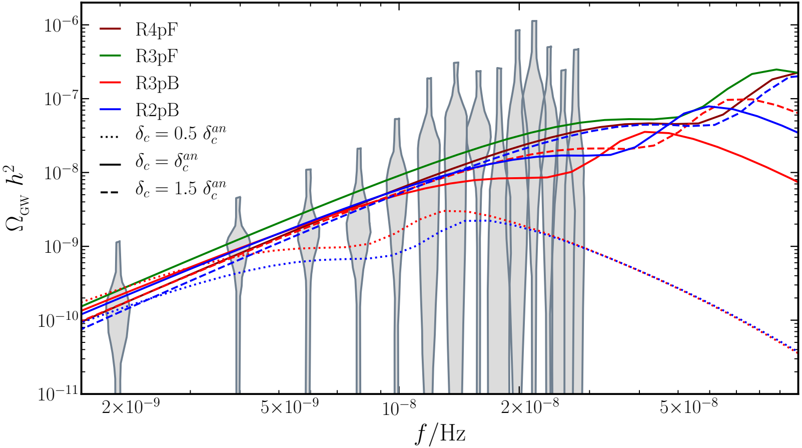

Epoch of reheating

The dimensionless spectral energy density of the secondary GWs today $\Omega_{\rm GW}(f)$ is plotted for a given reheating temperature and the best-fit values of the parameters in the different models[57].

[57] S. Maity, N. Bhaumik, Md. R. Haque, D. Maity and L. Sriramkumar, JCAP **01**, 118 (2025).

Power spectra and the extent of PBHs formed

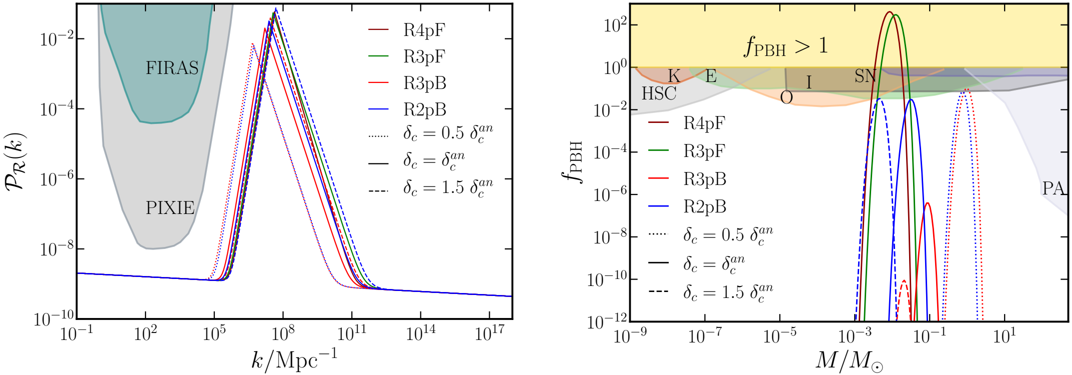

Scalar power spectra (on the left) and the extent of PBHs formed (on the right). We have assumed a specific reheating temperature and have plotted the fraction of PBHs that constitute the dark matter density today, viz. $f_{\mathrm{PBH}}(M)$, for the best-fit values of the parameters in the different models[58].

[58] S. Maity, N. Bhaumik, Md. R. Haque, D. Maity and L. Sriramkumar, JCAP **01**, 118 (2025).

Bayesian evidence for scalar-induced secondary GWs

Model X	Model Y	$\mathrm{BF}_{Y,X}$		
		$\delta_{\mathrm{c}} = 0.5\,\delta_{\mathrm{c}}^{\mathrm{an}}$	$\delta_{\mathrm{c}} = \delta_{\mathrm{c}}^{\mathrm{an}}$	$\delta_{\mathrm{c}} = 1.5\,\delta_{\mathrm{c}}^{\mathrm{an}}$
SMBHB	R2pB	$1.7 \pm .06$	260.04 ± 19.21	350.61 ± 27.36

The Bayesian factors $\mathrm{BF}_{Y,X}$ for the model `R2pB` that invokes primordial physics as the source of the stochastic GW background observed by the NANOGrav 15-year data, when compared to the astrophysical scenario that involves mergers of supermassive black hole binaries (SMBHB).

Bayesian factors $\mathrm{BF}_{Y,X}$ that far exceed unity indicate strong evidence for the model Y with respect to the model X.

Clearly, when $\delta_{\mathrm{c}} = \delta_{\mathrm{c}}^{\mathrm{an}}$ and $\delta_{\mathrm{c}} = 1.5\,\delta_{\mathrm{c}}^{\mathrm{an}}$, the NANOGrav 15-year data strongly favors the model `R2pB` when compared to the SMBHB model.

Plan of the talk

Outlook

- The increasingly precise observations of the CMB by future missions such as LiteBIRD (Light satellite for the studies of B-mode polarization and Inflation from cosmic background Radiation Detection), Primordial Inflation Explorer (PIXIE) and Exploring Cosmic History and Origin (ECHO, a proposed Indian effort) can be expected to help us improve the current constraints on the primordial correlations.
- The observations by LIGO are a culmination of almost fifty years of effort to detect GWs. They have opened up a new window to observe the universe.
- The observations by the PTAs and their possible implications for the stochastic GW background offer a wonderful opportunity to understand the physics operating in the early universe.
- Over the coming decades, GW observatories such as the Laser Interferometer Space Antenna, Einstein Telescope and Cosmic Explorer, can be expected to provide us with an unhindered view of the primordial universe.

The technical part of this talk was based on. . .

- M. Braglia, D. K. Hazra, F. Finelli, G. F. Smoot, L. Sriramkumar and A. A. Starobinsky, *Generating PBHs and small-scale GWs in two-field models of inflation*, JCAP **08**, 001 (2020) [arXiv:2005.02895 [astro-ph.CO]].
- H. V. Ragavendra, P. Saha, L. Sriramkumar and J. Silk, *Primordial black holes and secondary gravitational waves from ultra slow roll and punctuated inflation*, Phys. Rev. D **103**, 083510 (2021) [arXiv:2008.12202 [astro-ph.CO]].
- Md. R. Haque, D. Maity, T. Paul and L. Sriramkumar, *Decoding the phases of early and late time reheating through imprints on primordial gravitational waves*, Phys. Rev. D **104**, 063513 (2021) [arXiv:2105.09242 [astro-ph.CO]].
- H. V. Ragavendra and L. Sriramkumar, *Observational imprints of enhanced scalar power on small scales in ultra slow roll inflation and associated non-Gaussianities*, Galaxies **11**, 34 (2023) [arXiv:2301.08887 [astro-ph.CO]].
- S. Maity, N. Bhaumik, Md. R. Haque, D. Maity and L. Sriramkumar, Constraining the history of reheating with the NANOGrav 15-year data, JCAP **01**, 118 (2025) [arXiv:2403.16963 [astro-ph.CO]].

Collaborators I

Matteo Braglia

Dhiraj Hazra

Fabio Finelli

George Smoot

Alexei Starobinsky

H. V. Ragavendra

Pankaj Saha

Joseph Silk

Collaborators II

Md. Riajul Haque

Debaprasad Maity

Tanmoy Paul

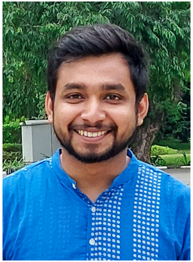

Suvashis Maity

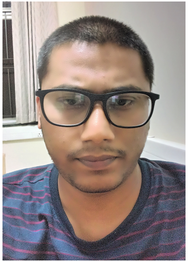

Nilanjandev Bhaumik

Thank you for your attention